16th World Congress in Computational Mechanics (WCCM)
21-26 July 2024, Vancouver, Canada
A. Korobenko, M. Laforest, S. Prudhomme, R. Vaziri (Eds)

ASSUMPTION BULGING FREQUENCY OF THE REAL SCALE TANK BY MICRO-TREMOR MEASUREMENT AND THE EIGENVALUE ANALYSIS

SHU HIRAI[1], TAISUKE ONO[2], HIROKAZU HIRANO[3] AND NAOTSUGU SATO[4]

[1]Chuo University
1-13-27 Kasuga, Bunkyo-ku, Tokyo 112-8551, Japan
a19.43mm@g.chuo-u.ac.jp

[2]NYK Co., Ltd
2-6-15 Kyobashi, Chuo-ku, Tokyo 104-0031, Japan
t.ono@nyk-tank.co.jp

[3]Chuo University
742-1, Higashi Nakano, Hachioji, Tokyo 192-0393, Japan
hirano@tamacc.chuo-u.ac.jp

[4]Chuo University
1-13-27 Kasuga, Bunkyo-ku, Tokyo 112-8551, Japan
nsato.57n@g.chuo-u.ac.jp

Key words: bulging, micro-tremor measurement, eigenvalue analysis, SUS tank, finite element method.

1 INTRODUCTION

Damage to tanks has been reported every time an earthquake with a seismic intensity of 6 or higher occurs, such as the 2011 Tohoku Pacific Coast Earthquake (Great East Japan Earthquake), the 2016 Kumamoto Earthquake, and the 2022 Fukushima Prefecture Earthquake.[1-5]. The damage assessment revealed that there are two main types of damage that can occur inside the tanks.

The first case is damage to the roof and upper sidewalls of the tank, and the second case is damage to the sidewalls and corners, mainly at the bottom of the tanks. The first is caused by the sloshing phenomenon (liquid level motion due to resonance between the natural frequency of the liquid content and the dominant frequency of seismic waves) due to longer-period seismic motion. On the other hand, the second type is caused by the bulging phenomenon[6,7] (coupled vibration between tank wall and liquid content), and is mainly caused by vibration of the tank structure due to short-period seismic motion.

For the sloshing phenomenon, the Housner's theoretical formula[8] has been used as a design standard. In contrast, the bulging phenomenon has just been newly stipulated in the "Guidelines and Explanations for Earthquake-Resistant Construction Methods for Water Facilities (Japan Water Works Association) 2022 Edition". Considering the elastic forces of the tank, it is essential to check the real scale tank bulging and devise a method to identify the tank bulging.

Since the bulging phenomenon is a coupled vibration between the sidewall and the liquid, it is most important to understand the natural frequency of the sidewall in order to determine

whether the bulging phenomenon is occurring. Therefore, we used the measurement method proposed by Saito et al[10]. In this case, we are using actual SUS panel tank whose sidewalls natural frequency is estimated to be less than 10.0 Hz. The sidewalls of SUS panel tanks have relatively low rigidity and are characterized by large deformations. It should be noted here that due to the presence of internal reinforcement, the stiffness of the sidewalls is significantly different from the stiffness of the reinforcement. Next, we perform eigenvalue analysis, which is identified as the natural frequency of the sidewalls determined from the spectrum obtained from the micro-tremor measurement and confirm consistency with the natural frequency of the mode that causes the bulging phenomenon. By comparing the natural frequencies obtained from both results, it is possible to estimate the natural frequency of the sidewalls of a real scale tank. This frequency is defined as the bulging natural frequency, and the possibility of a bulging phenomenon occurring can be determined. This method is intended for application to the investigation and inspection of seismic performance of real scale tanks.

2 CONCEPT OF TANK DESIGN CRITERIA

2.1 Concepts on sloshing phenomenon

In the sloshing phenomenon, it is assumed that the sidewalls of the tanks are perfectly rigid, and that the fluid motion in the tanks can be approximated by a simple physical model, represented by Housner's theoretical equation[8]. This model allows for the derivation of design approximation equations for the determination of seismic hydrodynamic pressure in rectangular and cylindrical tanks. Accordingly, the dynamic hydraulic pressure exerted on the sidewalls during an earthquake is a consequence of the rigid body motion of the tanks. Consequently, the pressure is proportional to the input acceleration.

2.2 Concepts on bulging phenomenon

The phenomenon of bulging is a consequence of coupled vibration between a fluid and a structure. This occurs when the sidewalls of the structure contact the liquid, causing them to vibrate while the sidewalls themselves deform as an elastic body. Consequently, it is regarded as a problem of coupled vibration of fluid and structure, which represents a distinct phenomenon from the sloshing phenomenon and exhibits complex behavior. The bulging phenomenon is not considered during the design process, which is likely to have resulted in a significant amount of damage.

2.3 Handling of natural frequencies around 10.0 Hz

In Ochiai's study[11], the ISSC (International Seismic Safety Centre) has adopted a method in which the effective acceleration of earthquake motion is between 0.5 Hz and 10.0 Hz. Acceleration above 10.0 Hz is not considered in terms of seismic strength. The high-frequency component of earthquake motion above 10.0 Hz is considered to have a limited effect on the seismic strength of structures, as its energy is relatively small, even if the acceleration response becomes significant. It is therefore postulated that seismic ground motions above 10.0 Hz are unlikely to cause damage to tanks. It is essential to determine whether the bulging phenomenon occurs at a frequency of 10.0 Hz. In addition, if the frequency is below 10.0 Hz, it is necessary to implement countermeasures such as installing a vibration control device [12].

3 TARGET TANK

In this study, micro-tremor measurements and eigenvalue analysis are conducted on the SUS panel tank shown in **Figure 1**. The tank in question is a two-tank unit with a width of 6000 mm, a depth of 3000 mm, and a height of 3000 mm per tank. For this reason, the structure is equipped with partition plates at the boundaries of the tanks. The interior of the tank is reinforced with SUS components in a complex configuration reminiscent of a jungle gym. Furthermore, the thickness of the panel wall of the tank is less than that of other steel plate tanks. Consequently, the tank exhibits low wall stiffness and a pronounced difference in stiffness between the reinforcement and the panel. The thicknesses of the plates are 2.5 mm for the first, 2.0 mm for the second, and 1.5 mm for the third wall. The base plate and annular plate are constructed from SUS304A, while the first and second rows of the wall are made from SUS444. The third row of the wall and the roof plate are composed of SUS329J4L. The measurements and analysis were conducted with the tank filled to a height of 2,700 mm, which represents 90% of the volume. **Table 1** shows the target tank specifications.

4 MICRO-TREMOR MEASUREMENT

4.1 Micro-tremor measurement device

For micro-tremor measurement, we employ the DATAMARK JU410 integrated micro-tremor measurement device, manufactured by Hakusan Kogyo Inc. and shown in **Photo 1**, which is proposed by Saito et al. [10]. The unit is an integrated system comprising a high-precision servo accelerometer. The device is lightweight (3 kg) and battery-powered, allowing for the seamless execution of measurements that necessitate agility. It can also be operated remotely via Wi-Fi.

In the study conducted by Saito et al.[10], a micro-tremor measurement device is installed on the roof to facilitate the continuous measurement of micro-tremor. Additionally, the apparatus is employed to quantify the vibration induced by a light tap on the wall surface with a hammer.

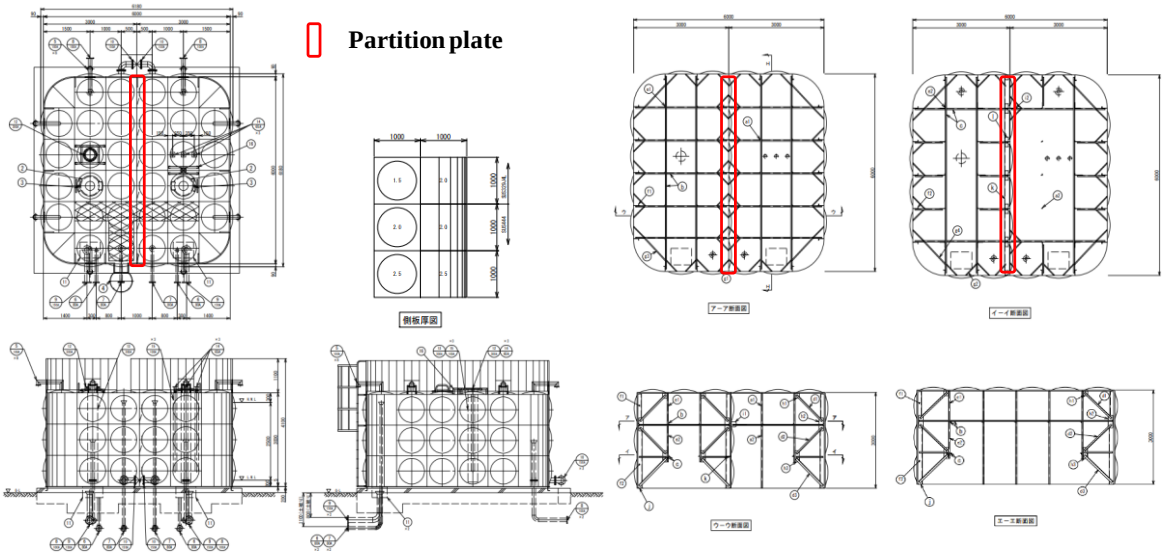

Figure 1: Drawing of target stainless steel panel tank

Table 1: Tank specifications

Material properties	Roof plate	SUS329J4L
	3rd side plate	SUS329J4L
	2nd side plate	SUS444
	1st side plate	SUS444
	Annular plate	SUS304A
	Base plate	SUS304A
Weight (mm)		6000
Length (mm)		6000
Height (mm)		3000
Effective capacity (m^3)		83
Water level (mm)		2700
Thickness (mm)	3rd side plate	1.5
	2nd side plate	2.0
	1st side plate	2.5

Photo 1: Micro-tremor measurement device

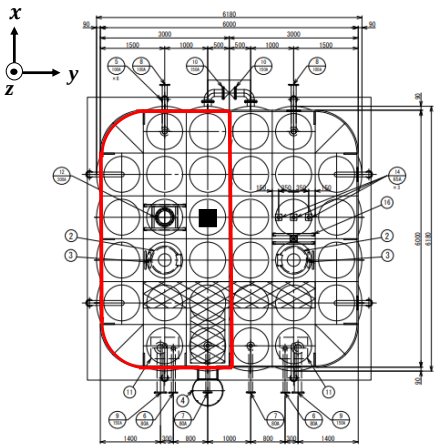

Figure 2: Micro-tremor measurement device installation position (■: Microtremor meter)

Table 2: Measurement conditions

	Measurement type
Case1	Micro-tremor measurement
Case2	Micro-tremor measurement when side wall are tapped

The micro-tremor measurement device is also employed to ascertain the bulging natural frequencies of the sidewalls. It has been demonstrated that this method can be employed to estimate the bulging natural frequencies of the sidewalls.

4.2 Measurement position

In this study, the tanks are considered as a single structure, with measurements taken on one side of the tanks. The micro-tremor measurement device is installed in a central position on the roof of the tank, as illustrated in **Figure 2** (the position indicated by the ■ mark). Each measurement is then performed.

4.3 Measurement contents

The measurements are conducted under the two conditions specified in **Table 2**. In Case 1, a constant micro-tremor measurement is conducted with the micro-tremor measurement device installed in the center of the roof. In Case 2, a micro-tremor measurement is conducted when the side wall surface is lightly tapped. The sampling frequency of the micro-tremor measurement device is 1000 Hz. The *x*-axis represents the direction perpendicular to the short side of the tank, while the *y*-axis represents the direction perpendicular to the long side. The *x* and *y* accelerations are then measured. The bulging phenomenon occurs when the side walls deform due to their elastic nature. Accordingly, in Saito et al.[10], the vertical direction, the *z*-axis direction, is not the direction of deformation of the sidewall and is therefore not considered in this study. For the purposes of this study, the *z*-axis direction is not considered.

4.4 Methods of analyzing measurement data

The response acceleration obtained from Case 1 and 2, along with the analysis range, are presented in **Figure 3** and **4**. In both case, those ranges are taken 30 seconds. In Case 2, the wall surface is lightly tapped after the commencement of the measurement, thus the beginning 10 seconds data is omitted to avoid the influence of foreld vibration and the damping state has reached a constant level. Consequently, the analysis range for Case 1 is 0 to 30 seconds, while that for Case 2 is 10 to 40 seconds. The range of bulging natural frequencies is assumed to be 0 to 20.0 Hz, which is twice 10.0 Hz importance upper limit as mentioned in **2.3**, to consider double vibration, and low-pass filtering is applied at 20.0 Hz.

4.5 The estimation method of natural frequencies

The natural frequencies of the sidewalls are estimated based on the results of the spectrum analysis. The estimation method is as follows.

(1) Check the most dominant frequency in the spectrum obtained from the Case 1 measurement. It should be noted that this may be the natural frequency of the reinforcement material placed inside the structure.
(2) Check the spectrum and dominant frequency of Case 2 in the *x* and *y* directions, respectively.
(3) Extract the one that agrees with the dominant frequency confirmed in (1) above.

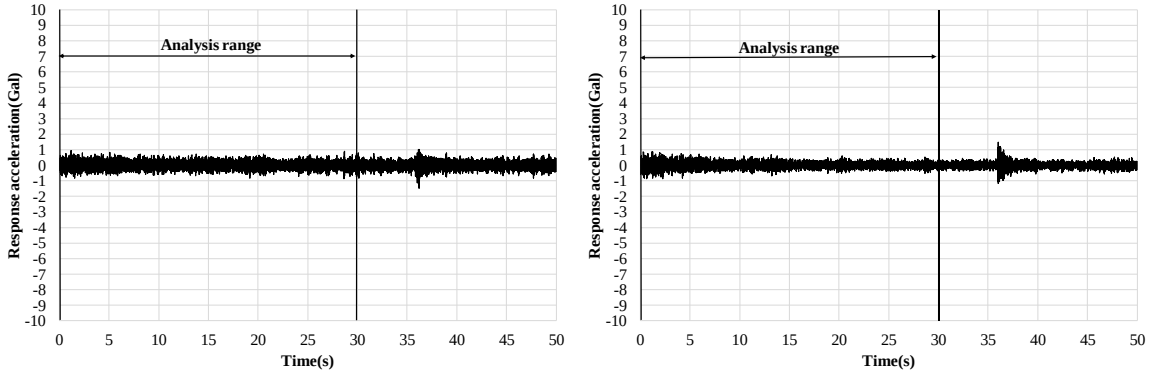

(a) *x* direction (b) *y* direction

Figure 3: Case 1 Response acceleration based on micro-tremor measurement (Constant micro-tremor)

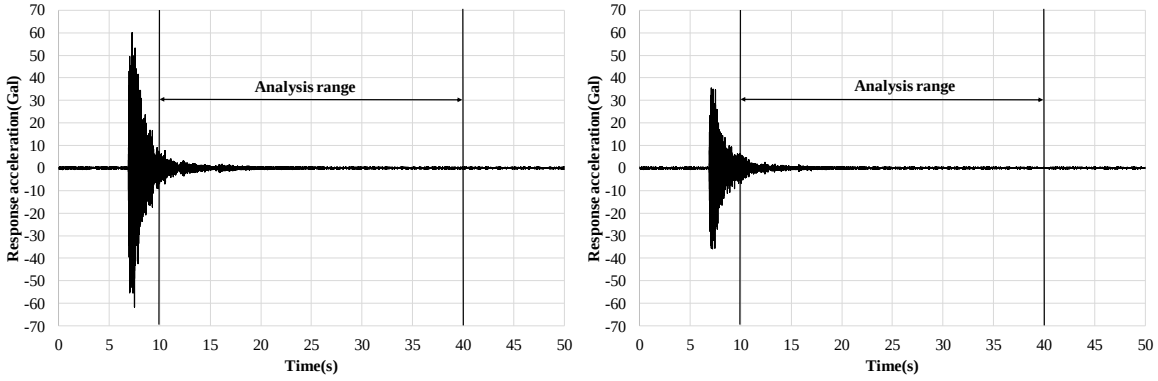

(a) *x* direction (b) *y* direction

Figure 4: Case 2 Response acceleration based on micro-tremor measurement (Tapping on the wall)

4.6 Results of analyzing measurement data

Figure 5, **6** show the results of spectral analysis of the response acceleration in the *x* and *y* directions for each measurement obtained from the micro-tremor measurement device installed on the roof of the tank.

Figure 5(a) illustrates that the most prevalent frequency in the *x* direction is 11.60 Hz, as measured by a micro-tremor device. This frequency is observed in Case 1. **Figure 6**(a) illustrates that the most dominant frequencies in the *x* direction are 11.54 Hz and 11.78 Hz in Case 2, where the wall surface is struck. The above results indicate that the natural frequencies of the short wall are likely to be in the range of 11.0 to 12.0 Hz, since the dominant frequencies in both cases are in the 11.50 to 11.60 Hz range.

Figure 5(b) illustrates that the most prominent frequency in the *y* direction is 4.46 Hz, as observed by the micro-tremor measurement in Case 1. **Figure 6**(b) illustrates that the predominant frequency in the *y* direction is 4.46 Hz in Case 2, where the wall surface is struck.

The above results indicate that the natural frequency of the longitudinal wall is likely to be in the 4.0 Hz range, since the predominance at 4.46 Hz is confirmed in all the measurements.

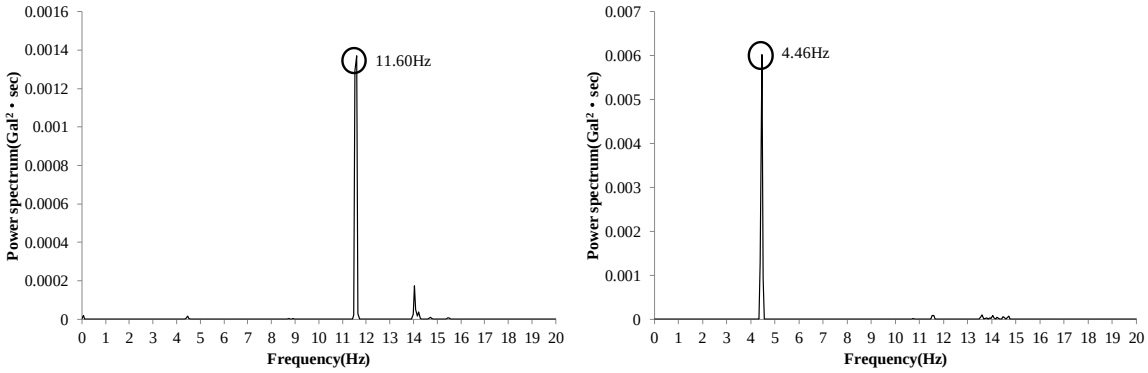

(a) *x* direction (b) *y* direction

Figure 5: Case 1 Spectrum analysis results from micro-tremor measurement

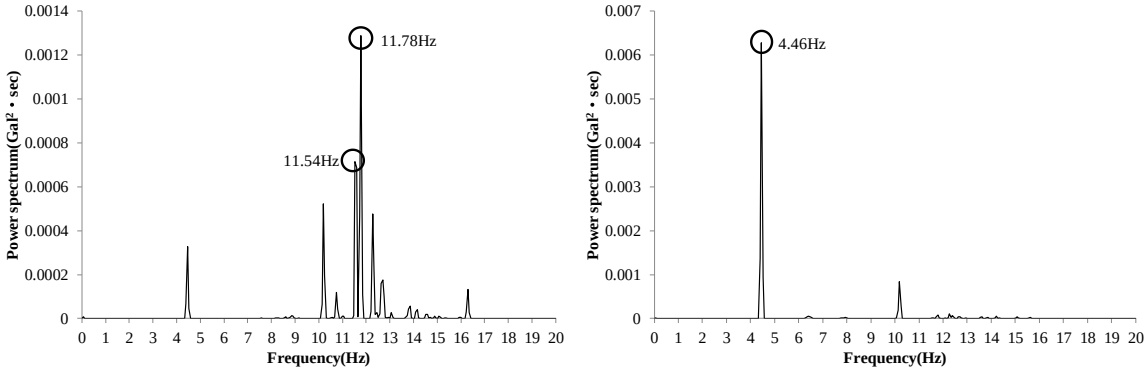

(a) *x* direction (b) *y* direction

Figure 6: Case 2 Spectrum analysis results from micro-tremor measurement

5 EIGENVALUE ANALYSIS

5.1 Analysis method

To compare the results with the measurement results, a natural frequency analysis of the target tank is performed. The general-purpose finite element analysis software ADINA is employed for this analysis. ADINA can analyze only the fluid component or can couple the fluid and structural problems together.

The analysis method is based on the authors' previous research[13] results, and the potential theory is applied to the fluid. The issue is represented as a coupled fluid/structure problem, with boundary conditions that maintain a uniform pressure at the wall surface, which is the structure, and at the fluid surface. To comprehend the quantitative phenomena, it is essential to accurately represent the structure-fluid interaction through a three-dimensional model and to employ the Navier-Stokes equations for the fluid analysis. However, this analysis requires a significant amount of computational time, necessitating the use of potential theory to gain a qualitative understanding of the phenomena. In particular, given that we are dealing with bulging phenomena, the fluid motion is not active, and thus the particle method is not employed in this analysis.

5.2 Governing equations

In the absence of rotational fluid motion and minimal wave surface deformation, the fluid motion is represented by a velocity potential φ, as described by the continuity equation in equation (1). The density ρ is assumed to be a constant value, given that incompressibility is assumed in this analysis.

$$\dot{\boldsymbol{\rho}} = \boldsymbol{\nabla} \cdot (\boldsymbol{\rho} \boldsymbol{\nabla} \boldsymbol{\varphi}) \tag{1}$$

The equation of motion presented in equation (2) and the boundary condition equation between the structure and the fluid presented in equation (3) are employed for the coupling of the fluid and the structure.

$$h = \Omega(x) - \dot{\varphi} - \frac{1}{2} \nabla\varphi \cdot \nabla\varphi \tag{2}$$

$$-\delta F_u = -\int_s pn\delta u dS \tag{3}$$

The specific enthalpy, h, is a function of pressure, p, and position, x. The body force acceleration at position x, $\Omega(x)$, is a function of the specific enthalpy, h, and the boundary, S. The force exerted on the structure by the fluid pressure on the boundary, S, is a function of the specific enthalpy, h, and the direction vectors, n and u.

5.3 Analysis outline

The model depicted in **Figure 7** is utilized in this analysis. **Figure 7**(a) illustrates the exterior of the tank, **Figure 7**(b) depicts the partition plate, and **Figure 7**(c) displays the internal stiffener. The x-axis is aligned with the short wall of the tank, the y-axis with the long wall, and the z-axis in the vertical direction. As illustrated in **Table 3**, the tank section is conceptualized as a shell element, the stiffener is regarded as a beam element, and the water surface is assumed to be a free surface. The fundamental equations employed are potential-based three-dimensional

fluid equations. During the mesh generation process, no nodal joints between the tank and the fluid are utilized to facilitate smooth surface behavior. The number of elements is 108,235, with 37,264 elements assigned to the tank, 2,627 elements to the reinforcement, and 68,344 elements to the fluid. The constraint conditions are fixed displacement and rotation of the bottom circumference and partition plate section. Eigenvalue analysis is performed at a frequency of 1 Hz in the range of 0 to 20.0 Hz as mentioned in **4.4**, with each frequency calculate in the range of 1000 modes.

In conventional eigenvalue analysis, the participation factor are calculated collectively within a defined frequency range. The natural frequency is defined as the point where the calculated participation factor exhibit significant values. However, when this method is employed in this study, the modes involved in the sloshing phenomenon dominate, resulting in a large stimulus coefficient. In contrast, the participation factor of the bulging mode is smaller than that of the sloshing mode. Consequently, the natural frequency of the bulging phenomenon has been overlooked because it is buried in the participation factor of the sloshing mode. Consequently, this study employs the methodology proposed by Takemoto et al.[14], wherein the eigenvalue analysis is repeated with finely divided intervals between the frequencies, as opposed to the conventional approach of lumped eigenvalue analysis with a wide predetermined frequency range. This method enables the calculation of the participation factor of the bulging mode, which is likely to be overlooked.

The natural frequencies of the sidewalls are verified by the following procedure, which is based on the participation factor calculated in this study.

(1) Check the participation factor in x and y directions and extract the participation factor that are larger than 10^{-4}.

(2) Calculate and confirm the mode diagram corresponding to the participation factor confirmed in (1).

5.4 Analysis results

The natural frequencies and participation factor, as determined by eigenvalue analysis, are presented in **Table 4**. The natural frequencies, calculated from the participation factor, are presented in **Figure 8**, along with the corresponding vibration mode diagrams. From **Table 4**

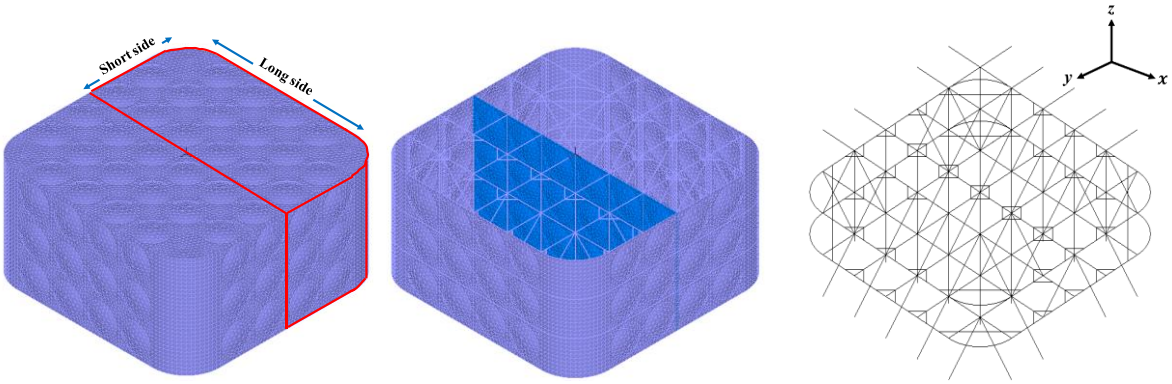

(a) Exterior of the tank (b) Partition plate (c) Internal stiffener

Figure 7: Analysis model of the target tank

and **Figure 8**(a), it can be concluded that the value of 4.82 Hz represents the natural frequency of the long wall (*y* direction). This is because the value of the participation factor in the *y* direction is considerable, and the mode occurs on the entire surface of the long wall (*y* direction). Similarly, the 4.91 Hz in **Figure 8**(b) exhibits a considerable participation factor in the *y* direction, with pronounced modes observed throughout the long wall (*y* direction) and partition plate, with a particular concentration in the lower portion of the sidewall. Previous studies[6, 7] have shown that damage to the sidewall of a tank caused by bulging often occurs at the base of the sidewalls. Based on the above, 4.91 Hz is the natural frequency of the long sidewall (*y* direction).

Figure 8(c) illustrates that at 5.89 Hz, a pronounced mode emerges on the long wall (*y* direction). The mode is also observed on the short wall (*x* direction) and at some point on the partition plate. Conversely, **Table 4** indicates that the participation factor in the *z* direction are more pronounced. **Figure 9** shows the vibration mode diagram at 5.89 Hz with the roof section added. **Figure 9** shows that a prominent mode is generated at the roof. This suggests that the mode may be indicative of the natural frequency of the roof of the tank, particularly in relation to the long wall surfaces. At 9.96 Hz in **Figure 8**(d), the mode occurs in both directions of the welds on the short wall, which is consistent with the natural frequency of the short wall (*x* direction). Given the near-identical locations of the mode generation and the welding area of the reinforcement in **Figure 1**, it is possible that the reinforcement's natural frequency may be reflected in this phenomenon. The value of 12.04 Hz in **Figure 8**(e) is the natural frequency of the short wall (*x* direction) due to the large value of the participation factor in the *x* direction and the occurrence of the mode on the entire short (*x* direction).

The 12.55 Hz value in **Figure 8**(f) exhibits considerable values of the participation factor in the *x* and *y* directions. The mode is observed to occur on the entire short-side wall (*x* direction) and a portion of the partition plate. The preceding analysis leads to the conclusion that the natural frequencies of the side walls are likely to be in the range of 12.55 Hz for the short side walls and 4.82 Hz and 4.91 Hz for the long sidewalls.

Table 3 Analysis conditions

	SUS304A	SUS444	SUS329J4L
Young's modulus（N/mm^2）	1.93×10^5	2.00×10^5	1.96×10^5
Density（kN/m^3）	79.3	77.5	78
Poisson's ratio	0.3		
Tank	Shell element		
Stiffner	Beam element		
Fluid	Potential 3D based fluid element		
Boundary condition	Edge displacement around the bottom and rotation fixation		
Fluid surface	Free surface		

Table 4 Natural frequencies and participation factor

Natural frequency(Hz)	Modal participation factor		
	x	*y*	*z*
…	…	…	…
4.82	5.18	2300.89	851.26
…	…	…	…
4.91	39.30	13518.40	-46.13
…	…	…	…
8.82	23837.30	70249800.00	9976440.00
…	…	…	…
9.96	15841000.00	560684.00	-258557.00
…	…	…	…
12.04	-116990.00	-369.68	134.99
…	…	…	…
12.55	6212510.00	768664.00	30554.30

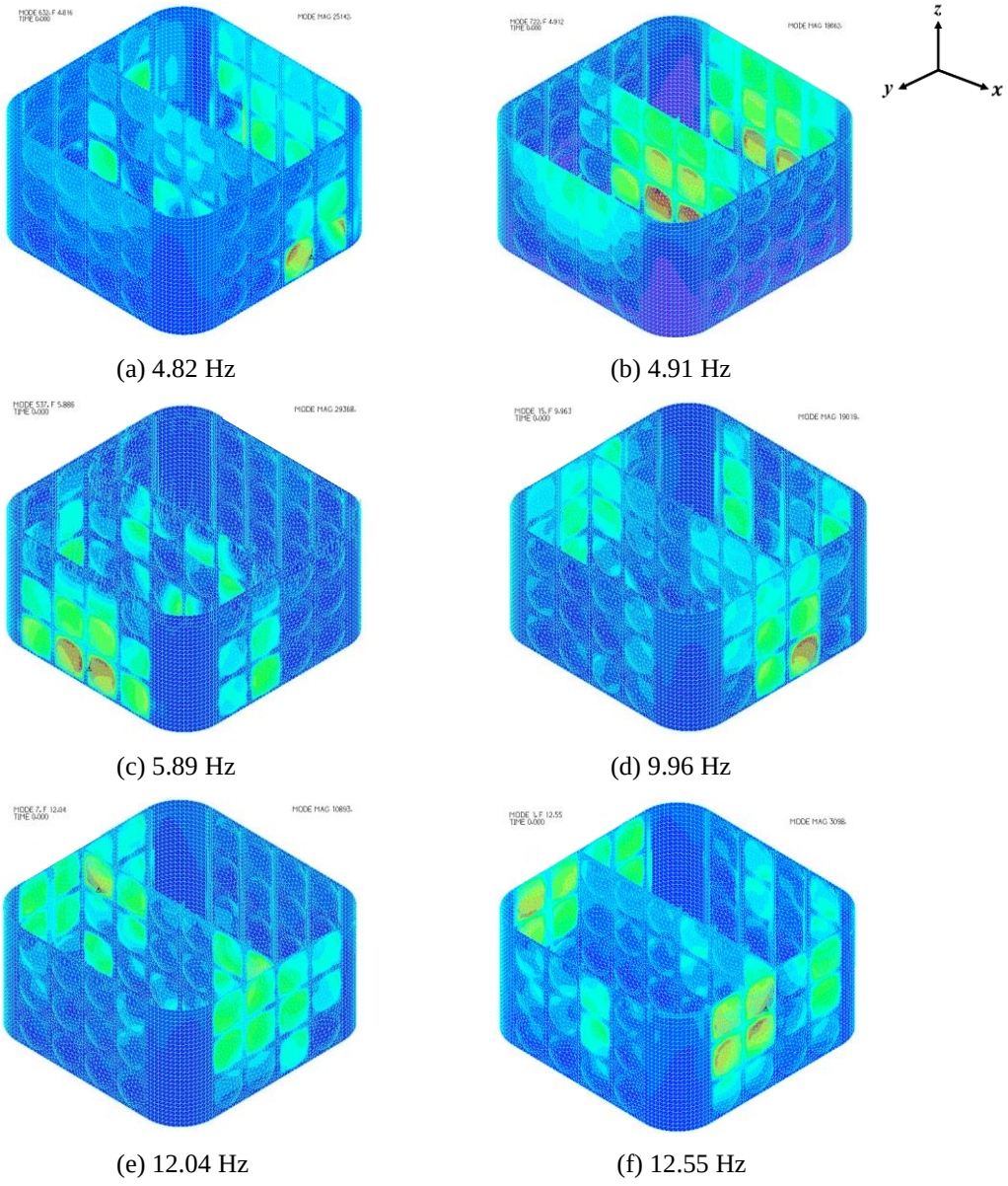

(a) 4.82 Hz (b) 4.91 Hz

(c) 5.89 Hz (d) 9.96 Hz

(e) 12.04 Hz (f) 12.55 Hz

Figure 8: Mode diagrams and natural frequencies

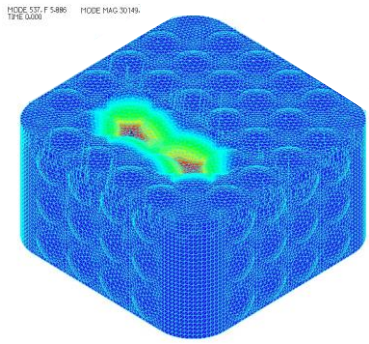

Figure 9: Mode diagram at 5.89 Hz (roof section)

6 COMPARISON OF MEASUREMENT RESULTS AND EIGENVALUE ANALYSIS

The micro-tremor measurement results presented in **Figure 6** indicate that the dominant frequencies are approximately 11.78 Hz and 4.46 Hz for the short wall (*x* direction) and long wall (*y* direction), respectively. Conversely, the results of natural frequency analysis also show 12.04 Hz and 12.55 Hz for the short wall (*x* direction) in **Figure 8**(e), (f), and 4.82 Hz and 4.91 Hz for the long wall (*y* direction) in **Figure 8**(a), (b), which are close to the results of micro-tremor measurement. The long side walls (*y* direction) in **Figure 8**(a), (b) have values of 4.82 Hz and 4.91 Hz, respectively, which are close to the results measured by the micro-tremor measurement. **Figure 8**(b) illustrates that the mode also occurs in the partition plate.

Based on the above, the natural frequencies of the side walls of the target tank are likely to be in the range of 4.0 to 5.0 Hz for the long side walls and 11.0 to 12.0 Hz for the short side walls. The natural frequency of the partition plate is also considered to be 4.0 to 5.0 Hz, which is equivalent to that of the long side wall.

The frequency of earthquakes in nature is generally less than 10.0 Hz, and even if it is higher, the energy of earthquakes is considered to be small[11]. Consequently, given that the natural frequency of the long sidewalls of the tanks in this study is less than 10.0 Hz, the natural frequency of the sidewalls is the bulging natural frequency. Accordingly, it is postulated that the installation of a vibration control device[12] would enhance seismic resilience.

7 CONCLUSIONS

In this study, the natural frequency of the sidewalls is calculated from the acceleration obtained from a micro-tremor measurement device equipped with a servo accelerometer. This is done using an actual SUS panel tank with a low stiffness sidewall and internal reinforcement, where the natural frequency of the sidewall is expected to be below 10.0 Hz. The natural frequencies of the tank are analyzed and compared with the measured results. The results of the measurement and analysis demonstrate a high degree of agreement between the values obtained from the micro-tremor measurements and those obtained from the eigenvalue analysis. The results presented above demonstrate that the measurement method[10] can be employed to ascertain the bulging natural frequencies of actual SUS panel tanks. In addition, since the measurement omits the labor, it can be applied to the investigation and inspection of the seismic performance of actual tanks. Accordingly, the natural frequencies of the sidewalls of the tank utilized in this study are estimated to be 4.0 to 5.0 Hz for the long sidewalls and 11.0 to 12.0 Hz for the short sidewalls. It can be reasonably inferred from the aforementioned data that the natural frequency of the long sidewall is below 10.0 Hz. Consequently, it is possible that bulging may occur on the long sidewall, requiring the installation of a vibration control device[12].

REFERENCES

[1] Ono, T., Enda, Y., Takemoto, J., Hirano, H. and Sato, N.: *Damage investigation of stainless steel panel tanks in the Kumamoto earth-quake and verification of damage during sloshing ocurrence*, Journal of Structural Engineering, A., Vol.66A, pp.137-146, (2020).

[2] The Water Supply Division of the Health Bureau of the Ministry of Health, Labor and Welfare.: *The Survey Report on Damage to Water Supply Facilities in the Great East Japan Earthquake (2011 Disaster Assessment Data Compilation Version)*, (2022).

[3] The National Institute for Building Research: *Fifth Investigation Report on Damage to Buildings and Other Structures Caused by the 2016 Kumamoto Earthquake (Preliminary Report)*, (2016).

[4] Inoue, R., Sakai, F. and Omine, S.: *Damage of water tanks and its relationship with strong ground motion in Kumamoto area during the 2016 Kumamoto earthquake*, Journal of Japan Society of Civil Engineers, Ser. A1 (Structural Engineering & Earthquake Engineering)., Vol.73, No.4, pp.711-720, (2017).

[5] The National Research Institute of Construction Science and Technology: A damage survey report for reinforced concrete buildings and facilities resulting from the earthquake off the coast of Fukushima Prefecture at 23:36 on March 16, 2022., 2023.

[6] Shionoya, R., Hirano, H., Ida, T. and Kawata, A.: *Vibration experiments on the bulging vibration of real scale water tank, Journal of Japan Society of Civil Engineers*, Ser. A1 (Structural Engineering & Earthquake Engineering)., Vol.73, No.4, pp.404-411, (2017).

[7] Ono, T., Take-moto, J., Ida, T., Hirano, H. and Sato, N.: *Comparison of bulging vibration response characteristics of real scale tanks with different structural form, Journal of Japan Society of Civil Engineers*, Ser. A1 (Structural Engineering & Earthquake Engineering)., Vol.76, No.4, pp.66-74, (2020).

[8] Housner, G.W.: *The dynamic behavior of water tank, bulletin of the seismological society of America*, Vol.53, No.2, pp.381-387, (1963).

[9] Japan Water Works Association: *Guidelines and Explanations for Earthquake Resistant Construction Methods for Water Supply Facilities 2022 Edition*, (2022).

[10] Saito, S., Ono, T., Ikeda, N., Hirano, H., Sato, N.: *Estimation the natural frequency of the bulging in water tank using the micro-tremor measurement device*, Journal of Structural Engineering, A., Vol.69A, pp.253-261, (2023).

[11] Ochiai, K.: *Capacity of NPPs against earthquake & proposals to prepare for post earthquake electric supply*, Journal of the Atomic Energy Society of Japan., Vol.56 No.2, pp.12-16, (2014).

[12] Ohno, S., Ono, T., Takemoto, J., Miyamoto, Y. and Hirano, H.: *Understanding of bulging vibration using non-earthquake resistant FRP water tank and examination of countermeasures*, Journal of Japan Society of Civil Engineers, Ser. A1 (Structural Engineering & Earthquake Engineering)., Vol.78, No.4, pp.511-522, (2022).

[13] Hirano, H., Matuda, H., Naganuma, H., Ida, T. and Tarukawa, T.: *Study of numerical analysis FSI method for sloshing vibration of floating-roof-tank*, Journal of Structural Engineering, A., Vol.53A, pp.605-613, (2007).

[14] Takemoto, J., Ono, T., Hirano, H. and Sato, N.: T*ime history response analysis of fluid and structure for stainless steel panel tank*, Journal of Japan Society of Civil Engineers, Ser. A2 (Applied Mechanics)., Vol.76, No.2, pp.153-162, (2020).